# Encapsulation in Poly(ethylene terephthalate)/Polyamide-6/Phenoxy Ternary Blends

Moo Sung LEE,[†] Min Gyu HA, Chang Nam CHOI, Kap Seung YANG, Jin Bong KIM, Taek Hyeon KIM, and Gi Dae CHOI[*]

*Faculty of Applied Chemistry and Advanced Materials Research Institute,
Chonnam National University, Kwangju 500–757, Korea
*LG Chemical Ltd., 84 Jangdong, Yusong Science Town, Taejon 305–343, Korea*

ABSTRACT: Ternary blends of Poly(ethylene terephthalate) (PET), Polyamide-6 (PA6) and phenoxy were prepared to compatibilize immiscible blends of PET and PA6. Phenoxy phase during melt mixing was characterized using electron microscopes, SEM and TEM. For PA6 matrix blends, it resided at the interface between PET and PA6 and forms an encapsulating layer during melt mixing. For PET matrix blends agglomerate particles were observed as a result of coalescence even though phenoxy encapsulated minor PA6 phase. The encapsulation of phenoxy onto PET or PA6 was interpreted in terms of a spreading concept combined with solubility parameter. Although phenoxy added as a compatibilizer does not stabilize the morphology it increases the tensile properties of PA6/PET blends.
KEY WORDS Polymer Blend / Encapsulation / Compatibilization / Poly(ethylene terephthalate) (PET) / Polyamide-6 (PA6) / Phenoxy /

Encapsulation by homopolymers may be an alternative for compatibilization of immiscible polymer blends when the preparation of compatibilizers such as block or reactive copolymers is not available. If a third polymer added moves to the interface between matrix and dispersed phase, and forms an encapsulating layer during melt mixing, it has potential to act as a compatibilizer.[1–4] This polymer should satisfy other prerequisites such as strengthening of the interface to become effective compatibilizer. Since simple encapsulation by third homopolymers generates two different weak interfaces between encapsulating polymer and matrix (or dispersed phase), the third must be carefully chosen to accomplish successful compatibilization.[5] This requirement may be one of the main reasons why encapsulation does not attract attention for compatibilization of immiscible polymer blends.

Whether the third polymer forms an encapsulating layer or not depends on two different factors. First, a thermodynamic factor such as interfacial tension has been considered the main driving force for encapsulation of ternary polymer blends. A third polymer added to immiscible polymer blends tends to move to the interface and encapsulate the minor phase when the sum of interfacial tension associated with the third is smaller than the interfacial tension between the original pair. A spreading coefficient, $\lambda_{ij}$, explains the importance of interfacial tension in the morphology of ternary polymer blends.[1] When polymer 3 is added to the immiscible blends of matrix polymer 1 and dispersed polymer 2,

$\lambda_{32}$ is defined as $\lambda_{32} = \gamma_{12} - [\gamma_{13} + \gamma_{23}]$, where $\gamma_{ij}$ is the interfacial tension of $i$ and $j$. If $\lambda_{32} \geq 0$, encapsulation of 3 onto 2 is expected in a given matrix. Most blends showing encapsulating structure are well predicted using $\lambda_{ij}$.

Kinetic factors such as melt viscosity affect final morphology irrespective of thermodynamic consideration. Nemirovski and coworkers[6] reported that when the viscosity of an encapsulating polymer, predicted from the interfacial tension difference, is higher than that of the minor phase, encapsulation is limited by high viscosity, thus balancing the thermodynamic driving force. Chemical reactions between blend components during mixing affect the morphology evolution of ternary polymer blends, as reported for ternary elastomeric blends.[7]

This study investigates the morphology of ternary blends of polyamide-6 (PA6), polyethylene terephthalate (PET), and poly(hydroxy ether of bisphenol A) (phenoxy) using electron microscopes. The blends are designed with the purpose of compatibilizing immiscible blends of PA6 and PET. From previous work on the compatibility of phenoxy with PA6 or PET,[8,9] it is expected that phenoxy be a compatibilizer for immiscible PA6/PET blends. Typical approach used for compatibilization of PA6/PET blends has been to add a catalyst -for example, *p-toluenesulfonic acid*- for accelerating the ester-amide interchange reaction between PA6 and PET chains.[10] The products formed by the reaction are assumed to act as compatibilizers. However, catalysts added cause degradation as well as exchange reaction, and thus we do not obtain the desirable me-

---

[†]To whom correspondence should be addressed.

chanical properties we may expect.

## EXPERIMENTAL

PA6 was obtained from Hyosung, Korea and has the glass transition temperature ($T_g$) and melting temperature ($T_m$) at 52 and 214°C, respectively. PET was obtained from Samyang Co., Korea and its $T_g$ and $T_m$ are 83 and 252°C, respectively. Phenoxy was obtained from Union Carbide Co. and has the $T_g$ of 84°C. Figure 1 shows the complex viscosity of the polymers measured at 280°C. Note that $|\eta^*|_{phenoxy} > |\eta^*|_{PA6}$ for all frequency range.

Melt blended samples were prepared using a homemade mini-molder. Mixing was done at 280°C for 5 min. Total amount of sample per batch was 2 g and rotor speed 170 rpm, corresponding to a maximum shear rate of $5 s^{-1}$.[11] The sample code 80/20/10 denotes 80 part PA6, 20 part PET, 10 part phenoxy by weight. Before mixing all polymers are milled in the form of powder and dried under vacuum at 60°C.

Morphology of blends was observed using a scanning or transmission electron microscopy. For TEM observation, sections of 80 nm thickness were microtomed at room temperature and stained for 60 min with vapor of 0.5% $RuO_4$ in water solution.[12] For SEM observation, cryofractured surfaces were smoothed with an ultramicrotome, etched with THF to remove the phenoxy phase, and then gold-coated. Thermal properties of the blends were measured using a differential scanning calorimeter (DSC), a Perkin–Elmer DSC-7. The data obtained during second scan was used for discussion. The tensile properties of the blends were measured using a Shimadzu autograph AGS-D according to ASTM D638 M. Crosshead speed was 20 mm min$^{-1}$.
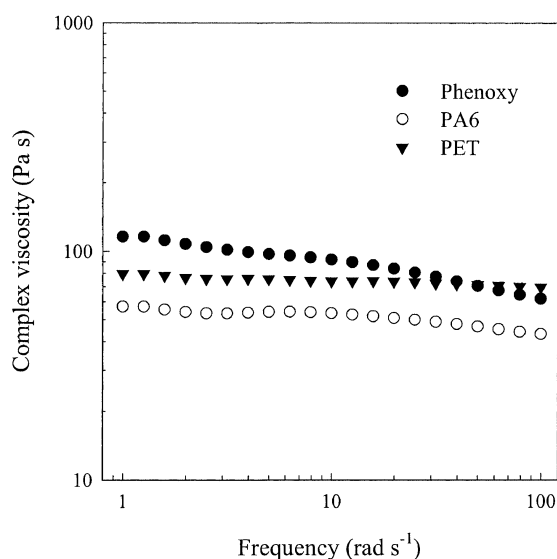
Infrared spectra were obtained using a Fourier transform infrared (FT-IR) spectroscopy in order to characterize the chemical reactions of phenoxy with PET or PA6. Two binary blends of 70/30 PET/phenoxy and 70/30 PA6/phenoxy, prepared under the same mixing conditions as for the ternary blends, were subjected to extraction with tetrahydrofuran (THF) for 1 h in a Soxhlet. Phenoxy is completely soluble in THF whereas PET and PA6 are insoluble. THF-soluble fractions were concentrated and cast onto KBr plates. After thorough drying, FT-IR spectra were obtained.

## RESULTS AND DISCUSSION

Figure 2 shows DSC thermograms of PA6/PET/phenoxy blends with and without phenoxy. Three characteristic transitions, $T_g$ of phenoxy at about 84°C, $T_m$ of PA6 at about 210°C, and $T_m$ of PET at about 250°C, are clearly seen for all of the ternary blends, indicating that three distinct phases exist in the blends. The tran-
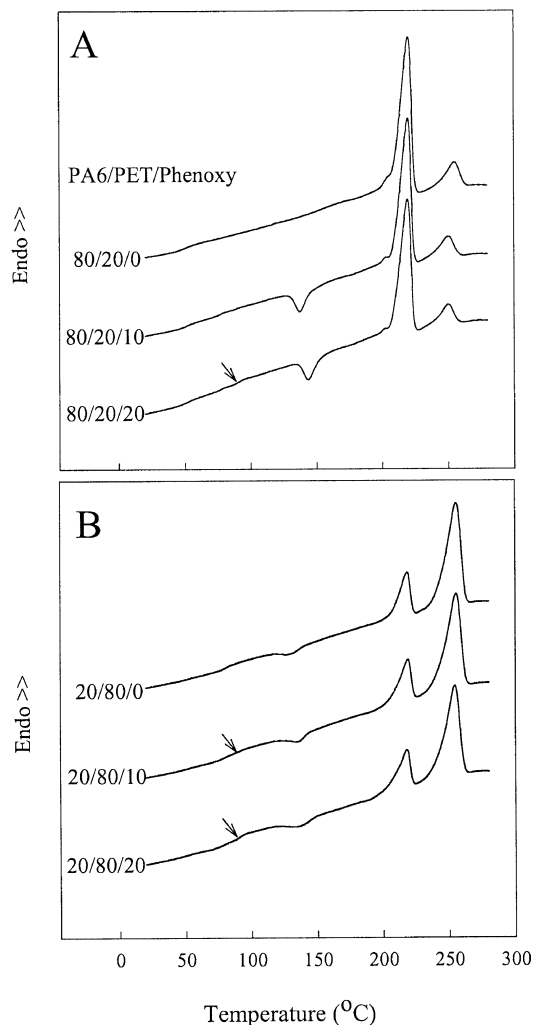
**Figure 2.** DSC thermograms of PA6/PET/phenoxy ternary blends: (A) PA6 and (B) PET matrix blends, respectively. Arrow indicates the $T_g$ of phenoxy phase.

**Figure 1.** Melt viscosities of polymers at 280°C.

**Figure 3.** SEM micrographs of (A) 80/20/20 and (B) 20/80/20 PA6/PET/phenoxy ternary blends.
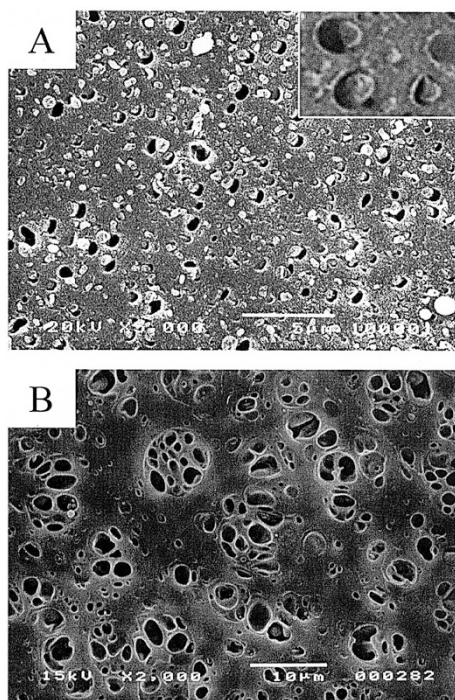


**Figure 4.** TEM micrograph of (A) 80/20/20 and (B) 20/80/20 PA6/PET/phenoxy ternary blends.

sitions remain unchanged compared with those of pure polymers. The phenoxy fraction dissolved in PA6 or PET phases during melt mixing is negligible to affect the thermal properties.

In order to be identified as a compatibilizer, it should move to the interface between matrix and dispersed phase during melt mixing and reside there. Figure 3 shows SEM micrographs of PA6/PET/phenoxy blends with different matrices. Since phenoxy phase was etched with THF, the craters in the figures correspond to the locations of phenoxy in the blends. For PA6 matrix blend, phenoxy encapsulates the minor phase of PET. For PET matrix blends, agglomerates of minor phases of PA6 and phenoxy make it difficult to figure out which polymer encapsulates which polymer. The location of phenoxy within agglomerate particles can be clearly seen in TEM micrographs.

Figure 4 shows TEM micrographs of PA6/PET/ phenoxy ternary blends. Comparing SEM and TEM micrographs in Figures 3A and 4A, it is clear that phenoxy is more stained than PA6 and appears darker under the staining conditions applied in this study. For PA6 matrix blend, encapsulation of phenoxy onto PET is clearly observed, as seen in Figure 4A. For PET matrix blend, a unique morphology, similar to the salami structure of high impact polystyrene, is observed. The salami-like structure corresponds to agglomerates observed in the SEM micrograph. By carefully examining the morphology of Figure 4B, we can find that the phenoxy phase, which appears dark, always forms the outer
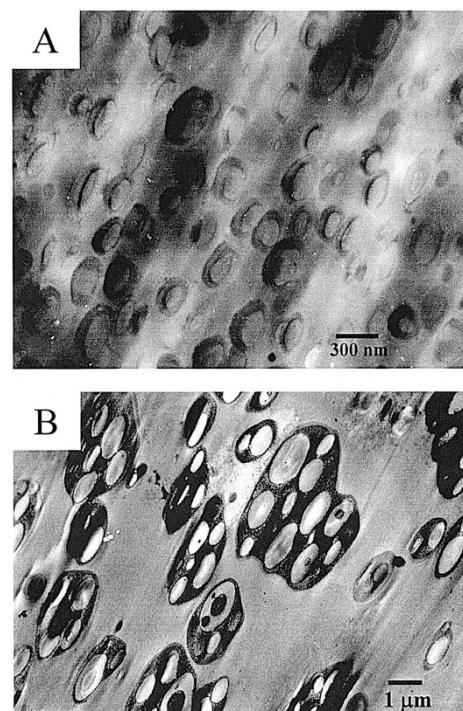
layer for all particles. Therefore, it is believed from the SEM or TEM micrographs that phenoxy has a thermodynamic tendency to encapsulate the minor phase of PET or PA6 during melt mixing.

Encapsulation of phenoxy onto PA6 or PET may be explained using wetting theory mentioned in the Introduction. Even though it is not possible to directly determine the spreading coefficient, $\lambda_{ij}$ because interfacial tension data between blend pairs are not available, we may calculate it using the solubility parameter, $\delta$, of blend components.[7] According to a mean-field theory,[13] $\gamma_{ij}$ is proportional to the square root of the Flory–Huggins interaction parameter $\chi_{ij}$. Since $\chi_{ij}$ is proportional to the difference in solubility parameters of blend component, $|\delta_i - \delta_j|$,[14] we approximate $\lambda_{32}$ and $\lambda_{23}$ as follows

$$\lambda_{32} = \gamma_{12} - [\gamma_{13} + \gamma_{23}] \approx |\delta_1 - \delta_2| - [|\delta_1 - \delta_3| + |\delta_2 - \delta_3|]$$
$$\lambda_{23} = \gamma_{13} - [\gamma_{12} + \gamma_{23}] \approx |\delta_1 - \delta_3| - [|\delta_1 - \delta_2| + |\delta_2 - \delta_3|]$$
(1)

Only when $\lambda_{32} \geq 0$ and $\lambda_{23} < 0$, encapsulation of 3 onto 2 in matrix 1 occurs. From eq 1 we deduce that component 2 has thermodynamic tendency to form encapsulating layer when $\delta_2$ is between $\delta_1$ and $\delta_3$, *i.e.*, $\delta_1 < \delta_2 < \delta_3$ or $\delta_3 < \delta_2 < \delta_1$. $\delta$ for PET, phenoxy and PA6, calculated using the Hoftyzer–Van Krevelen method,[15] are 19.58, 19.86, and 20.40 $J^{1/2} cm^{-2/3}$, respectively. Therefore, we predict that phenoxy has a thermodynamic tendency to encapsulate PA6 in PET matrix or PET in PA6 matrix. Although the prediction from solubility parameter is well consistent with the morphology
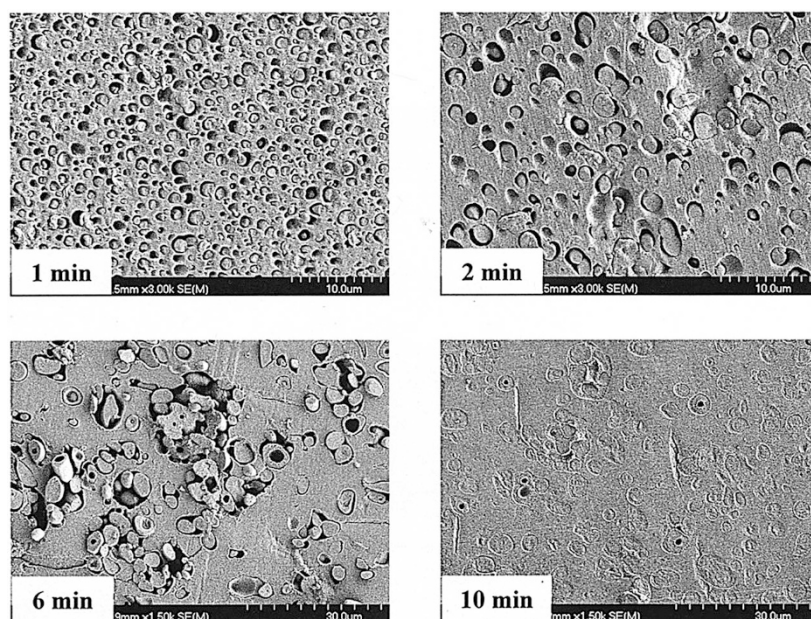
**Figure 5.** SEM micrographs of 20/80/20 PA6/PET/phenoxy ternary blends, mixed during different mixing time.

observed in this study, we should understand that $\delta$ estimated from group contribution method has some uncertainty. Chemical reaction between blend components changes interfacial properties and thus makes it difficult to predict the encapsulating morphology in equilibrium.

Figure 5 shows SEM micrographs of 20/80/20 PA6/PET/phenoxy blends with effect of mixing time on the agglomeration of dispersed domains. The blends were prepared under the same mixing conditions as for the blends of Figure 3, except mixing time. The blend mixed for 1 min shows typical dispersed morphology, in which phenoxy forms encapsulating layer and/or is dispersed as droplets in the PET matrix. As mixing time increases further, coarsening of dispersed particles occurs and agglomerate particles are formed. In the micrograph of 2 min mixing time two or more particles coalesce each other and then become larger. This indicates that encapsulating layer of phenoxy does not prevent dynamic coalescence during melt mixing. Salami-like structure and/or the phenoxy domain trapped in PA6 phase are clearly seen in the blend mixed for 6 min. For the blend mixed for 10 min the outer encapsulating layer of phenoxy is not effectively etched with THF due to the reaction with PET and thus we can not clearly see the contour of agglomerates. However, the phenoxy phase isolated in PA6 phase is etched and clearly seen. Figure 5 shows that the salami-like structure in the PET matrix blend results from coalescence of encapsulated particles during melt mixing. A factor, which prevents coalesced particles from rearranging into fused ones, should exist in the PET matrix blend. One possibility is chemical reactions between blend components, espe-
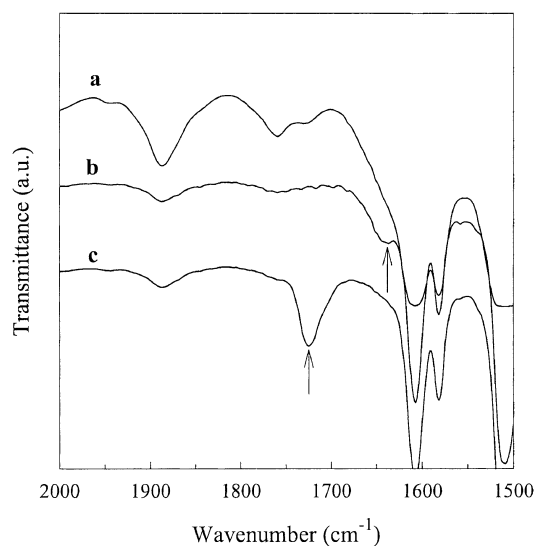


**Figure 6.** FT-IR spectra of neat phenoxy and binary blends with PET or PA6: (A) neat phenoxy; (B) 70/30 PA6/phenoxy blend; (C) 70/30 PET/phenoxy blend.

cially between PET and phenoxy.

Figure 6 shows FT-IR spectra of pure phenoxy and THF-soluble fractions of 70/30 PET/phenoxy and 70/30 PA6/phenoxy blends. Whether a chemical reaction between phenoxy and PET or phenoxy and PA6 occurs during melt mixing or not can be confirmed from the presence of the carbonyl stretching vibrations of PET or PA6. Since only phenoxy is soluble in THF and it does not contain any carbonyl group in chain, the existence of the carbonyl peak indicates that chemically linked polymers are formed by reaction during melt mixing. As shown in Figure 6, a new peak at $1724\,\mathrm{cm^{-1}}$ is observed for 70/30 PET/phenoxy blend, indicating the chemical reaction between PET and phe-
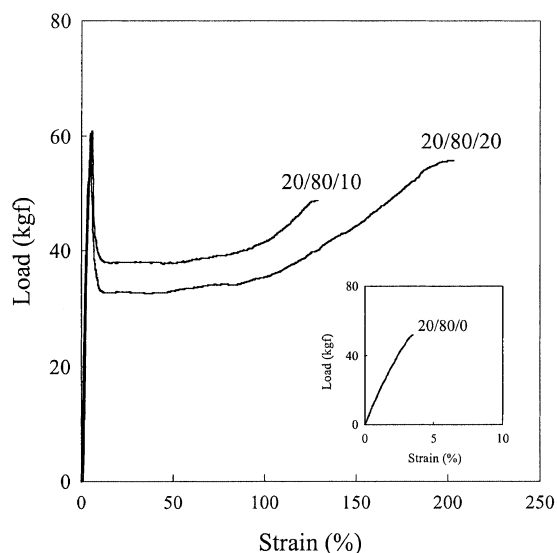
**Figure 7.** Load-strain curves of PET matrix blends. The insert represents a blend without phenoxy.

noxy. The reaction may reduce interfacial tension between PET and phenoxy and make the phase contact between them favorable. For 70/30 PA6/phenoxy blend a new peak corresponding to the amide I mode is observed around $1640 \, cm^{-1}$ but intensity is very small. Even though the reaction between phenoxy and PA6 occurs during mixing, the degree was not significant under the mixing conditions in this study.

Whether the encapsulating layer of phenoxy contributes to strengthen the interface or not can be inferred from the tensile properties of polymer blends. Weak interface will cause brittle fracture of polymer blends. Figure 7 shows the load-stain curves of PET matrix blends. Tensile tests, made at least 3 times under the same conditions, produced similar trends. The blend without phenoxy shows typical brittle fracture behavior. Phenoxy changes the fracture behavior from brittle to ductile fracture. It is believed that enhanced properties are caused by the adhesions between PA6/phenoxy and PET/phenoxy interfaces. Adhesions may originate from the compatibility between PA6 and phenoxy and from the chemical reactions between PET and phenoxy.

## SUMMARY

Ternary blends of polyamide-6 (PA6), polyethylene terephthalate (PET), and poly(hydroxy ether of bisphenol A) (phenoxy) were prepared using a mini-molder. Irrespective of matrix type phenoxy encapsulated minor phases, even though for PET matrix blends, a salami-like structure was observed as a result of coalescence during mixing. The encapsulation of phenoxy onto PA6

or PET could be interpreted in terms of spreading coefficient combined with solubility parameter. Combining the Helfand–Tagami equation for $\gamma_{ij}$ and Hildebrand's solubility parameter approach, we can predict that phenoxy, which has solubility parameter between those of PET and PA6, forms the encapsulating layer. Although a chemical reaction between PET and phenoxy took place during melt mixing and thus a copolymer was formed at the interface between PET and phenoxy, the reaction or resultant polymer does not stabilize the morphology. Tensile properties of ternary blends with phenoxy is enhanced compared to those without phenoxy. From the morphology and tensile properties of PET/PA6/phenoxy blends phenoxy clearly shows the possibility to act as an effective compatibilizer for immiscible PET/PA6 blends.

## REFERENCES

1. S. Y. Hobbs, M. E. J. Dekkers, and V. H. Watkins, *Polymer*, **29**, 1598 (1988).
2. S. Horiuchi, N. Matchariyakul, K. Yase, and T. Kitano, *Macromolecules*, **30**, 3664 (1997).
3. M. S. Lee, T. P. Lodge, and C. W. Macosko, *J. Polym. Sci., Part B: Polym. Phys.*, **35**, 2835 (1997).
4. H. F. Guo, S. Packirisamy, N. V. Gvozdic, and D. J. Meier, *Polymer*, **38**, 785 (1997).
5. J. Noolandi, in "Polymeric Materials Encyclopedia", J. C. Solomone, Ed., CRC Press, Bocca Raton, FL, 1996, vol. 9.
6. N. Nemirovski, A. Siegmann, and M. Narkis, *J. Macromol. Sci., Phys.*, **B34**, 459 (1995).
7. Y. Koseki, M. S. Lee, and C. W. Macosko, *Rubber Chem. Technol.*, **72**, 109 (1999).
8. L. M. Robeson and A. B. Furtek, *J. Appl. Polym. Sci.*, **23**, 645 (1979).
9. Y. S. Soh, *Polymer*, **35**, 2764 (1994).
10. L. Z. Pillon and L. A. Utracki, *Polym. Eng. Sci.*, **24**, 1300 (1984).
11. B. Maxwell, *SPE Journal*, **28**, 24 (1972).
12. J. S. Trent, J. I. Scheinbeim, and R. R. Couchman, *Macromolecules*, **16**, 589 (1983).
13. E. Helfand and Y. Tagami, *J. Polym. Sci., Polym. Lett. Ed.*, **9**, 741 (1971).
14. J. H. Hildebrand and R. L. Scott, "The Solubility of Nonelectrolyte", 3rd ed., ACS Monograph Series, Washington, D.C., 1950.
15. D. W. Van Krevelen, "Properties of Polymers", Elsevier Science Inc., New York, N. Y., 1990.